MCT Detectors and ROICs for Various Format MWIR and LWIR Arrays

Vyacheslav V. Zabudsky*, Fiodor F. Sizov*, Vladimir P. Reva**, Alexandr G. Golenkov*, Yuriy P. Derkach**, Sergei V. Korinets**, Ihor O. Lysiuk*, V.V. Vasiliev***, S.A. Dvoretsky***

*V. Lashkariov Institute of Semiconductor Physics, Kiev 03028, Nauki Av. 41, Ukraine
Fax: (380)-44-5258342, e-mail: sizov@isp.kiev.ua,
**Institute of Microdevices, Kiev, Ukraine
***A.V. Rzhanov Institute of Semiconductor Physics, SB RAS, Novosibirsk, Russia

ABSTRACT

Silicon ROICs for MCT LWIR (4x288, 6x576) and MWIR (128x128) diode matrix arrays were designed, manufactured and tested. MCT layers were grown by MBE technology on (013) GaAs substrates with CdTe/ZnTe buffer layers (λ_{co} = 11.2 ± 0.15 μm at T = 78 K) and by LPE technology on (111) CdZnTe substrates with HWE passivation layer.

The mean detectivity obtained e.g. for 4×288 FPAs at T = 78 K and background temperature T_b = 295 K was $D^*_\lambda \cong 1.8\times10^{11}$ cm·Hz$^{1/2}$/W with st. dev. ≈ 16.5 % (at FOV = 32°) and NEDT = 9.0 mK for the arrays tested and are close to the BLIP regime. NEDT measured for 128x128 FPA was about 20±8 mK.

1. INTRODUCTION

FPAs on the base of mercury-cadmium-telluride (MCT) today are the most widespread devices for 3-5 μm and 8-12 μm IR region with ultimate performance (see, e.g., Refs. [1, 2]). Since early ninetieths of the last century, when SOFRADIR proposed high resolution scanned arrays with time delay and integration (TDI) function and signal processing (first with charge coupled devices (CCD) for readouts) within the focal plane for standard TV formats resolution using mechanical scanning and odd and even line interlacing (576x768 European format), this type of FPAs became popular [2, 3] and there were produced high quantities of them. Here our experience in design of 4x288 readout devices (ROICs), fabricated by difference technologies, and some features of MCT FPAs on their base, will be stated. Some details concerning design and properties of 6x576, 128x128 will be mentioned too.

For 3 – 5 micron region staring matrix arrays with comparable dimensions to TV format and even in the case of lower quantum efficiency, have clear advantages over scanning arrays even with TDI function (see, e.g., [4, 5]), but for 8 – 12 micron spectral region they are of comparable effectiveness, and scanning arrays can be more cost effective.

2. ROICs DESIGN AND THEIR BASISIC CHARACTERISTICS

Different types of ROICs were designed and manufactured for 4×288 MCT arrays with the dimensions of photodiode sensitive cells of approximately 25×28 microns. The circuit was composed according to the block-diagram model shown in Fig. 1.

The number of outputs N depends on resources of instrumentation used for signal managing, first on ACD resources, and defines the multiplexor capacity. The number of TDI stages between the inputs is chosen from the needs of space resolution. In the circuits stated three stages were chosen.

For manufacturing of readouts three types of technology were used.

1) 2.5 μm n-MOS (n-type metal-oxide-semiconductor) + CCD (charge coupled devices) technological process with two levels of polysilicon electrodes and one metallization level.

2) 2.0 μm CMOS (complementary metal-oxide-semiconductor) + 2.5 μm CCD (charge coupled devices) technological process with two levels of polysilicon electrodes and two metallization levels.

3) Standard 1.0 μm CMOS technological process with two levels of polysilicon and two metallization levels.

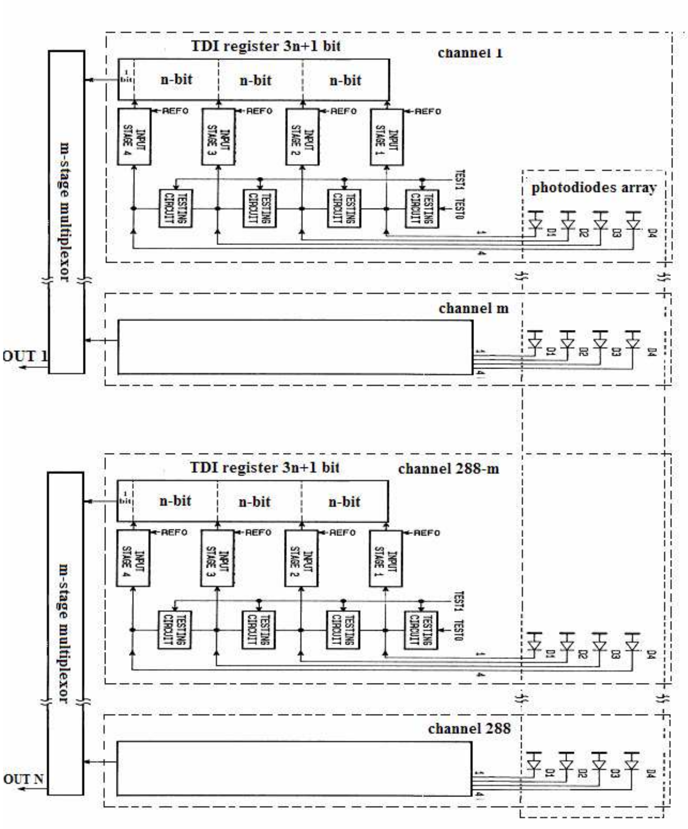

Fig.3. Block-diagram of 4x288 ROIC.

In all circuits for improving of the coupling between PV detector and readout device there were chosen the unit cells with direct injection (DI). DI transistor characteristics are important for read-out device performance. To ensure the minimum characteristics dispersion for direct injection transistor there was used "natural" transistor, which did not include the additional operations of channel doping. Besides, DI transistor was designed of rather large area. It ensured in all the circuits designed the characteristics deviation within 10 mV. For maintenance of linear transfer characteristics was chosen transistor with channel length enough to exclude dependence of direct injection transistor current on drain voltage. In all circuits the testing elements are embedded to provide the possibility of multiplexers testing without connecting to photodiodes. Comparative parameters of the technologies used and ROICs designed are presented in Tables 1-3.

Table 1. Some comparative parameters of technologies used at fabrication of 4x288 ROICs.

Main parameters	Type of technology		
	2.5 µm (NMOS+ CCD)	2.0µm CMOS+ 2.5µm CCD	1.0µm CMOS
Wafer	Four-inch boron-doped *p*-type <100>12 Ohm×cm	Four-inch boron-doped *p*-type <100>12 Ohm×cm	Six-inch boron-doped *p*-type <100>12 Ohm×cm
Number of photo-masks	9	14	11
Thickness of under-gate dielectric,	450 ± 50 A	350 ± 50 A	250 ± 15 A
Threshold voltage nature transistor	0.3 ± 0.15 V	0.3 ± 0.15 V	0.15 ± 0.05 V
Channel width	2.5 µm	2.4 µm	1.2 µm

Silicon ROICs for MCT LWIR 576×6 diode matrix arrays with TDI function were designed and manufactured too. They include 576×6 array of LWIR MCT detectors with TDI function 4 blocks of 144x6 arrays with 56x43 micron pixels. Diodes shift perpendicular to scanning direction is 0.25 of pixel size. ROICs were designed for their manufacturing by 0.6 micron design rules CMOS technology with 2 polysilicon levels and 2 metal levels. Six elements TDI function is used with bidirectional scanning, "dead" elements deselection, gain trim control, image data format and integration time selection, 8 levels input capacity programming, direct testing of the PV sensitive elements was also included. Max input capacity is 2.7 pC, the capacity at the TDI output register is about 2.0 pC, the output signal amplitude is not less than 2.8 V, the dynamic range is 77 dB. There are 8 video outputs, and the frequency range is 5 MHz.

Table 2. Basic parameters of ROICs

Parameter	ROIC type		
	NMOS-CCD	CMOS-CCD	CMOS
Structure(Nxm)	16x18	4x2x36	4x72
Input stage	DI, analog 2 capacitor stage with anti-blooming and background skimming	DI, analog 2 capacitor stage with anti-blooming and background skimming	DI, digital 2 capacitor stage with anti-blooming and background skimming
Testing stage	Controlling testing transistor	Controlling testing transistor	Testing transistor include in trigger deselection
Pixel random deselecting	no	yes	Yes
TDI	CCD register 4 input 3 bit between input 10 bit total	CCD register 4 input 3 bit between input 10 bit total	Reverse BBD register 4 input 3 bit between input 10 bit total
multiplexor	18 bit CCD	36 bit CCD	Sample and hold amplifier
Output stage	Source follower	Operation amplifier	Operation amplifier
Additional functions	No	Yes, pixel random deselecting	Yes, pixel random deselecting; reverse TDI scan; 8-range gain adjustment; bypass testing; main-clock based internal time sequence.

Table 3. Basic parameters of ROICs

Parameter	ROIC type					
	n-MOS-CCD				CMOS-CCD	CMOS
	2 phase	4 phase	buried channel	surface channel		
Maximum input charge integration capacity	6.4 pC				4.0 pC	4.48 pC
Using range of adjustment input capacity	0.2 – 5.0 pC				0.2 – 4.0 pC	8 digital stage 0.56, 1.12,…4.48 pC
Charge handling capacity of TDI register	2.0 pC	2.4 pC	2.2 pC	2.6 pC	3 pC	2.2 pC
Output rate of video signal	2 MHz	2 MHz	2 MHz	2 MHz	4 MHz	5.5 MHz
Maximum output signal	≥5 V	≥5 V	≥5 V	≥6 V	≥3 V	≥2.5 V
dynamic range	≥60dB	≥65dB	≥65dB	≈70dB	≥70dB	≥77dB
noise	≤5 mV	≤4 mV	≤2 mV	≤2 mV	≤1.5 mV	≤400μV
Geometrical noise(difference between channel for dark level)	≤4 mV	≤2 mV	≤2 mV	≤2 mV	≤2 mV	≤100 mV
Non-linearity	≤5%	≤4%	≤3%	≤2%	≤2%	≤1%
Electrical cross-talk	<5%	<4%	<4%	<5%	<10%	<1%
Power dissipation	≤50mW	≤50mW	≤50mW	≤50mW	≤100mW	≤80mW

CMOS readout devices for MCT MWIR (3-5 µm) 128x128 diode matrix arrays were designed and manufactured as well. ROIC include (see Fig. 2):

1. The input cells with pads, which provide the attachment to photodiodes, accumulation and photocurrent transformation into voltage;
2. Column amplifiers;
3. Buffer storage amplifier;
4. Scanning multiplexers;
5. Video output amplifier;
6. Digital manager which produce all the necessary signals of scanning control, delivering to the output the signals of the row onset (start), frame, synchronization of the outside ADC.

Readout device consists from matrix of 128x128 input stage with 2 columns of "black or dark cells" (that provided "level of black"), column amplifiers, digital interface, that include all necessary block for formed need internal and outside signal.

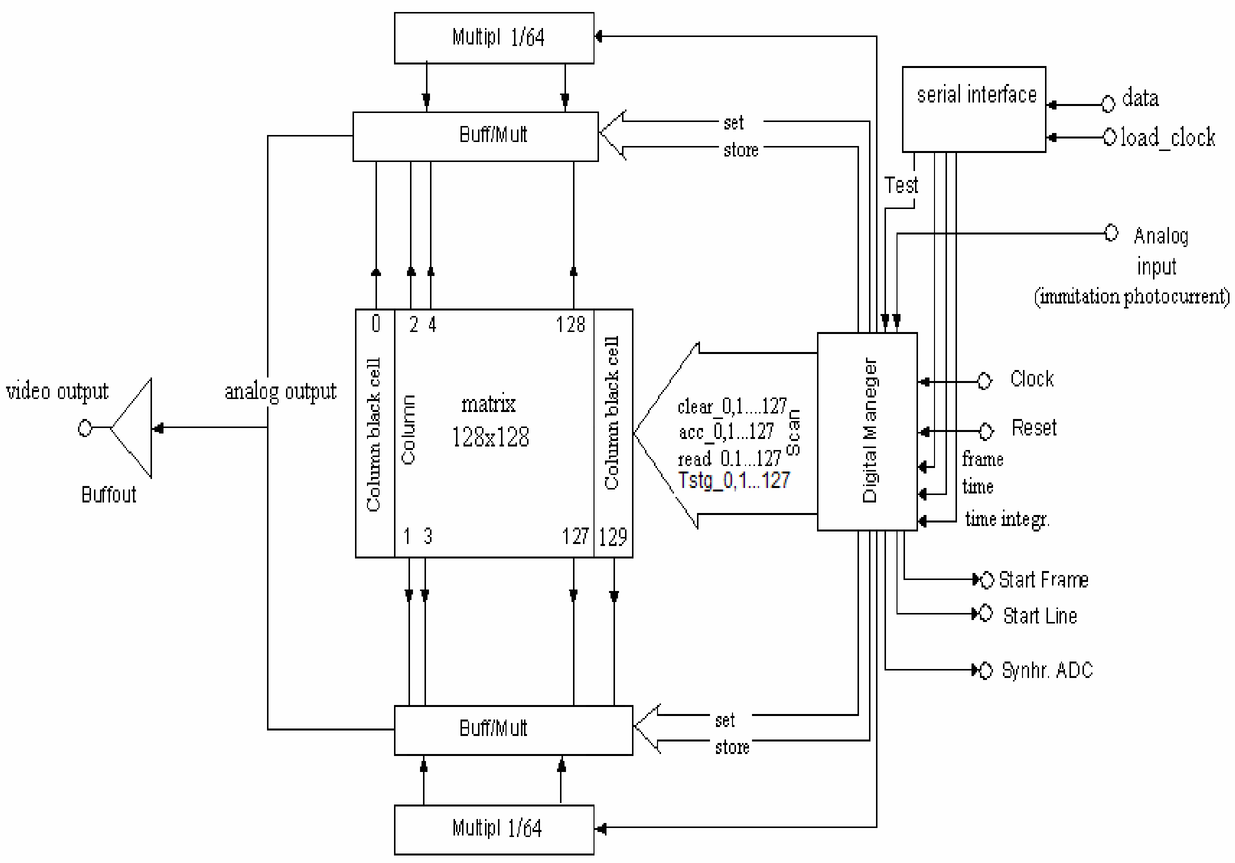

Block circuit readout 128x128.

Fig. 2. Block diagram of 128x128 readout device.

Readout devices have four regime of functioning.

1. Working regime – standard regime, when readout is working with matrix of photodiodes, provided video picture with needed scan frequency
2. First test regime, when testing elements provide input current to input cells, instead photodiodes and all matrix scanning. (Testing possibility without connection to photodiodes array).
3. Second test regime, when testing elements provide input current to input cells, instead photodiodes, only one of line is access (number of line is setting by serial interface).
4. Third test regime, when readout will be checking with matrix of photodiodes, and only one of line is access (number of line is setting by serial interface).

For producing multiplexer it was used 1.0 CMOS technology with two levels of polysilicon and two levels metal. The parameters of ROICs are as following: maximum input charge integration capacity — 1.8 pQ, numbers of outputs — 2, clock rate — up to 10 MHz, frame rate — up to 200 Hz, output voltage — more than 2.5 V, integration time - 50 ~ 1000 μs, nonlinearity — less than 2%.

In Fig. 3, 4 the typical measured charge-voltage transfer characteristics for 4x288 and 128x128 ROICs are presented.

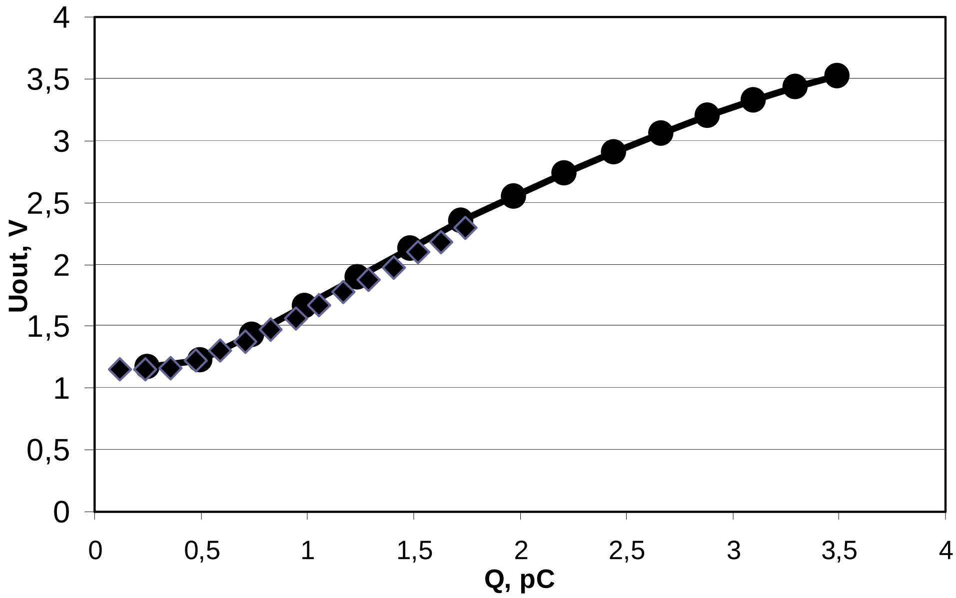

Fig. 3. Transfer characteristic of 4x288 multiplexer.

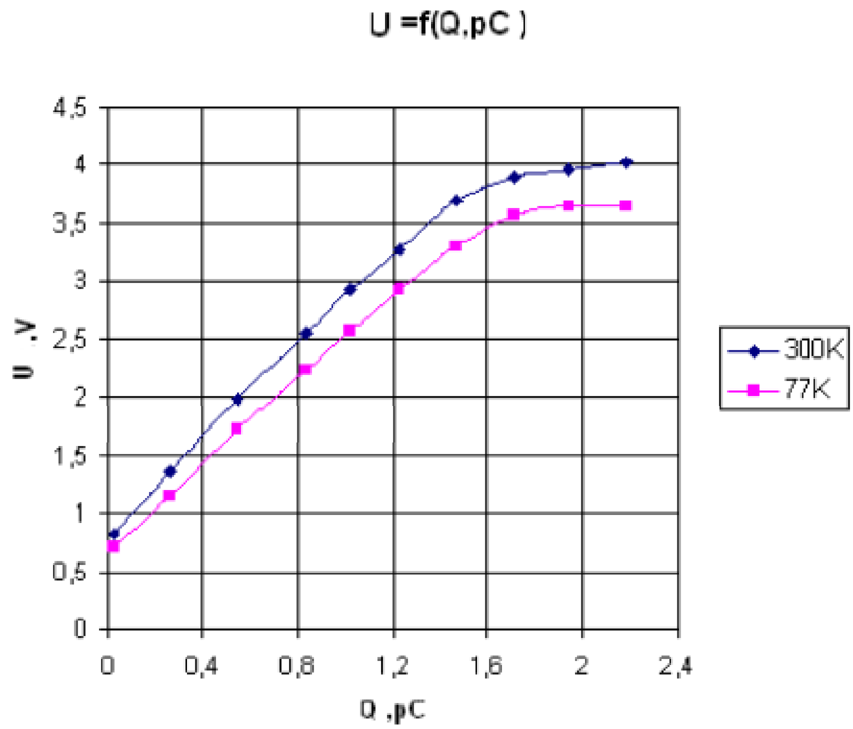

Fig. 4. Transfer characteristic of 128x128 multiplexer.

2. LWIR and MWIR PHOTODIODES PROPERTIES

The ultimate performance results of MCT traditional photovoltaic detectors, cooled down to temperature 77 K, for 3–5 and 8–14 µm spectral ranges were achieved. It is shown [6] by comparison of experimental data and modeling of I-V dark current characteristics that MCT photodiode characteristics are limited by diffusion current in n^+–n^-–p junctions and by current via the deep traps in the gap with position E_t= 0.7 E_g above the valence band and concentrations N_t = (1.0-5.5)·10^{15} см$^{-3}$ which are comparable with donor concentration in n^-–region N_d = (1.1-1.8)·10^{15} cm^{-3}. Charge transport mechanisms at reverse current depend on energies and doses of implanted boron ions.

The measured typical and modeled I-V characteristics of several photodiodes in linear arrays with TDI function or matrix arrays are shown in Fig. 6. Chemical depth composition dependence in the layers grown by MBE procedure and sensitivity spectral dependence of these photodiodes are shown in Fig. 5. It is evident from the spectral sensitivity dependence that in such kind of photodiodes one can evidently exclude the use of an additional cold spectral filter in FPA.

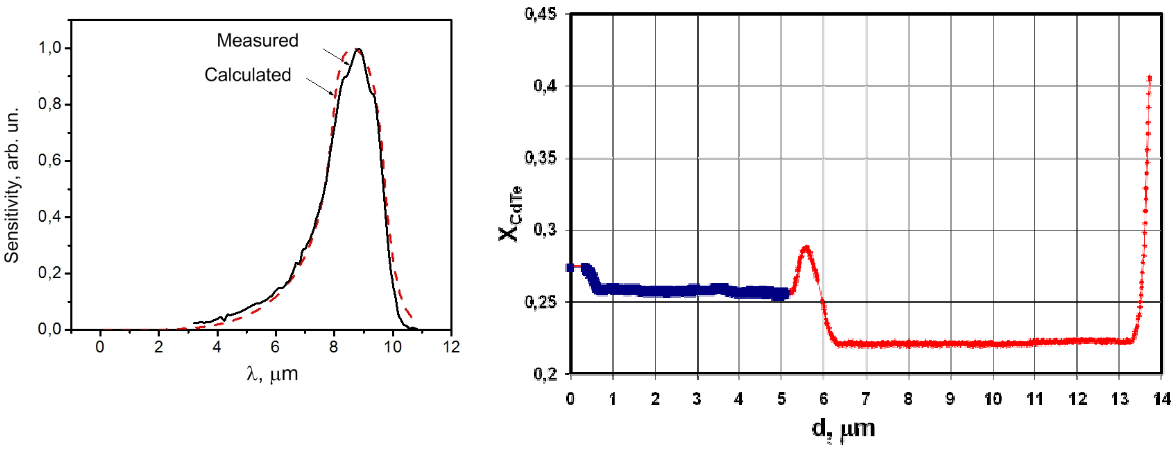

Fig. 5. Spectral dependence of LWIR photodiodes with chemical composition profile as shown right.

The photodiodes were manufactured with using both MBE and LPE technologies. The dark currents of 30 photodiodes (MBE) chose by random sampling in the 4x288 arrays with λ_{co} ≈ 10.3 µm have the mean dark current value I_{dc} ≈ 5.3 nA (T = 77 K) with deviation σ ≈ 16 %. The similar dark currents were measured in the best photodiodes manufactured from LPE layers. In the best MBE photodiodes the dark currents were at the level of I_{dc} ≈ 3 nA.

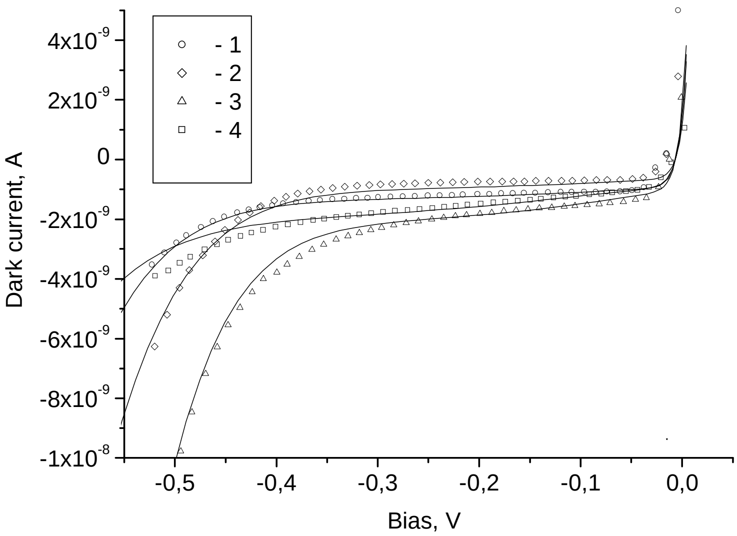

Fig. 6. Experimental (1, 2, 3, 4) and calculated (solid lines) dark current I-V-characteristics of several LPE grown $Hg_{1-x}Cd_xTe$ (x ≈ 0.215, λ_{co}≈10.3 µm) photodiodes from different parts of the array. T = 77K.

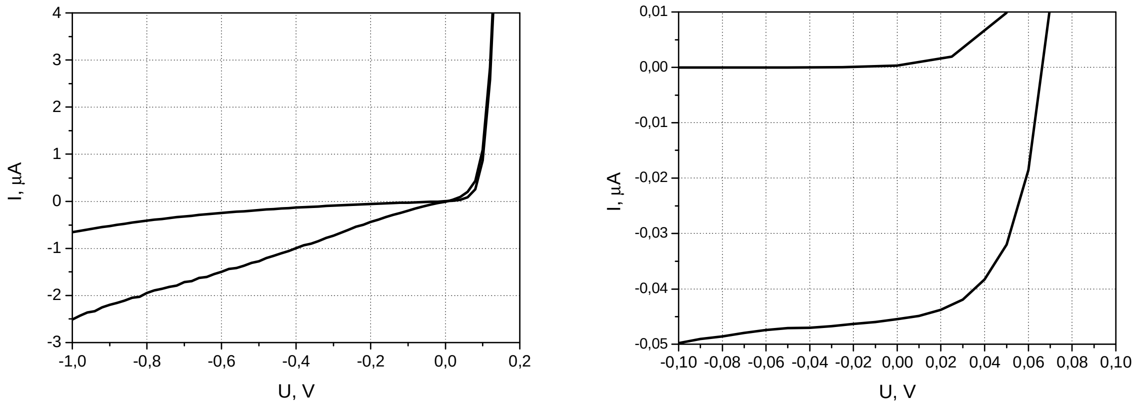

Fig. 7. Experimental dark (1) and background illuminated (2) I-V-characteristic of diode from matrix 128x128, based on $Cd_xHg_{1-x}Te$ (x≈0,3) at T=80 K. Left picture corresponds to LPE grown structures and right image — to MBE manufactured diodes.

In Fig. 7 are shown typical I-V-characteristics of diode from matrix 128x128, based on $Cd_xHg_{1-x}Te$ (x≈0,3) at T=80 K, manufactured by LPE (left) and MBE technique (right).

3. FPAs PROPERTIES

For measuring of ROICs and FPA parameters the testing equipment was developed. It can operate with various format ROICs and FPA (2x64, 4x288, 6x576, 128x128, 320x256, etc.) in automatic or part manual mode and provide measurements of maximum output signal, maximum charge, nonlinearity and nonuniformity of output signal, dark signal, signal noise, output signal dynamical range, ROIC power consumption, FPA detectivity, sensitivity and NETD.

The 288×4 and 128x128 IR FPAs was fabricated by hybrid assembling of photosensitive array and ROIC with the help of In bumps welding technology. In Fig. 8 (left) is shown the sensitivity distribution along one of the 4x288 linear arrays tested. Switching on the deselection function to dead elements in the channels allows one to exclude the presence of dead elements or defective channels in the FPA. For any ROICs used the mean detectivity obtained for all 4×288 FPAs with skimming mode included at T = 80 K, and background temperature T_b = 295 K, was in the range of $D^*_\lambda \cong (1.2 - 1.7)\times10^{11}$ cm·Hz$^{1/2}$/W for several arrays tested (at FOV=32°). The noise equivalent difference temperature for array with (CCD + CMOS) readout was $NEDT \approx$ 9 mK. For FPAs with other ROICs this parameter was of similar order. The dynamic range for arrays tested was about 75 dB. In the Fig. 8 (right) NEDT histogram for 128x128 FPA is presented. NEDT measured for 128x128 FPA was about 20±8 mK.

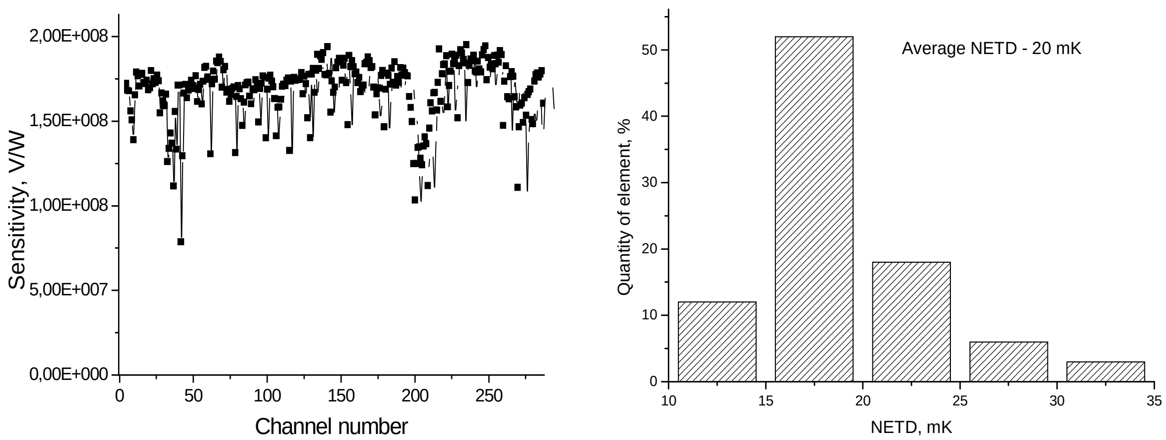

Fig. 8. Sensitivity distribution along 4×288 linear array with deselection function switch on. The NEDT histogram for 128x128 FPA.

4. CONCLUSIONS

Silicon ROICs for MCT LWIR (4x288, 6x576) and MWIR (128x128) diode matrix arrays were designed, manufactured and tested. It provides good parameters and functionality, for example reverse TDI scan, pixel random deselecting, anti-blooming and background skimming, bypass testing, testing without connect to photodiodes and control via serial and parallel ports. Silicon multiplexers were manufactured by different technology and the final one was 1.0 µm CMOS technology with two levels of poly-silicon and two metal levels.

MCT layers for LWIR and MWIR spectral region were grown by MBE and LPE technology. The dark currents of high quality LWIR diodes is equal to I=4-7 nA at reverse voltage bias U=150 мВ and was limited mainly by diffusion current.

The IR FPA were fabricated by In bumps hybrid assembling of photosensitive arrays and ROICs. The responsivity and detectivity mean values were equal to $S_V=2{,}27\times10^8$ V/W and $D^*_\lambda=2{,}13\times10^{11}$ $cm\times Hz^{1/2}\times W^{-1}$, respectively for 4x288 LWIR FPA. NEDT measured for 128x128 MWIR FPA was about 20±8 mK.

5. REFERENCES

1. *Rogalski A.* Infrared Detectors. Gordon and Breach Science Publishers (2000).
2. Chamonal J.-P., Mottin E., Audebert P., Ravetto M., Caes M., Chatard J.-P., “Long linear MWIR and LWIR HgCdTe arrays for high-resolution imaging”, *Proc. SPIE*, **v. 4130**, p. 452 – 462 (2000).
3. Tribolet Ph., Chorier Ph., Manissadjian A., Costa P., Chatard J-P., “High performance infrared detectors at Sofradir”, *Proc. SPIE*, **v. 4028**, p. 438 – 456 (2000).
4. Runciman H. M., “Influence of technology on FLIR waveband selection”, *Proc. SPIE*, v. 2470, p. 156 – 167 (1995).
5. *Holst J. C.* Electro-Optical Imaging System Performance. Bellingham, USA: SPIE Optical Engineering Press, 2003. – 442 p.
6. Gumenyuk-Sychevskaya J.V., Vasil’ev V.V., Dvoretskii S.A., Zabudsky V.V., Lusyuk I.A., and Michailov N.N. Current transfer mechanisms in MBE grown heteroepitaxial photodiode structures for 8-12 spectral region. XX Intern Conf. on Photoelectronics and Night Vision Devices, Moscow, p. 145 (2008) (In Russian).